Scientia Iranica F (2014) 21(3), 1183–1196

SCIENTIA IRANICA

Sharif University of Technology
Scientia Iranica
Transactions F: Nanotechnology
www.scientiairanica.com

Research Note

Nonlinear pull-in instability of boron nitride nano-switches considering electrostatic and Casimir forces

A. Ghorbanpour Arani[a,b,*], A. Jalilvand[a], M. Ghaffari[a], M. Talebi Mazraehshahi[a] R. Kolahchi[a], M.A. Roudbari[a] and S. Amir[a]

a. *Faculty of Mechanical Engineering, University of Kashan, Kashan, Iran.*
b. *Institute of Nanoscience & Nanotechnology, University of Kashan, Kashan, Iran.*

Received 16 December 2012; received in revised form 17 May 2014; accepted 12 July 2014

KEYWORDS
BNNB;
Pull-in instability;
Nano-switch;
NEMS;
Casimir force.

Abstract. Pull-in instability of Boron Nitride Nano-Beam (BNNB) under the combined electrostatic and Casimir force as nano-switch is presented. Using Euler-Bernoulli Beam (EBB) theory, nonlocal piezoelasticity theory, von Kármán geometric nonlinearity and virtual work principle, the nonlinear governing differential equations are obtained. The equations are discretized by two types of numerical methods, namely the Modified Adomian Decomposition (MAD) method and Differential Quadrature Method (DQM). Analysis of lower pull-in voltage values is considered for nano-switches with different boundary conditions. The detailed parametric study is considered, focusing on the remarkable effects of nonlocal parameter, beam length, boundary condition, geometrical aspect ratio and gap distance on the behavior of the pull-in instability voltage. The obtained results of DQM and MAD are compared with published relevant study. This work is hoped to be useful in designing and manufacturing of Nano-Electro-Mechanical Systems (NEMS) in advanced applications such as high-tech devices and nano-transistors with great applications in computer industry.

1. Introduction

BNNBs have the same atomic structure such as Carbon Nano-Beams (CNBs) but many interesting properties including a more stable electronic property and better resistance to oxidation at high temperatures ($\geq 900°$C) and possessing strong piezoelectric characteristics are concerned [1]. They were introduced in the middle of 1990s similar to CNBs as regards to high elastic modulus and super structural stability. BNNBs are therefore considered as a promising material to be employed as sensors and actuators, due to their unique structural, mechanical, thermal, electrical and chemical properties. Elastic properties of Boron Nitride Nano-Tubes (BNNTs) and Boron Nitride Nano-Sheet (BNNS) are reported by Oh [2].

Song et al. [3] proposed an atomistic-based continuum theory for BNNTs based on interatomic potentials for boron and nitrogen to study the Young's modulus, stress-strain curve and onset of bifurcation in Single-Walled Boron Nitride Nanotube (SWBNNT) under tension.

In recent years, a large amount of research works have been carried out on the buckling and vibration of the nano-beam in various structure and condition.

*. *Corresponding author. Tel: +98 31 55912450; Fax: +98 31 55912424*
E-mail addresses: aghorban@kashanu.ac.ir, and a_ghorbanpour@yahoo.com (A. Ghorbanpour Arani)

In order to demonstrate the mechanical modeling of these structures, the higher-order continuum theories, such as partial nonlocal elasticity, exact nonlocal elasticity, nonlocal piezoelectricity, modified couple stress, strain gradient elasticity and surface elasticity theory have been recently employed. Based on the partial nonlocal elasticity theory, Ghorbanpour Arani et al. [1] investigated the buckling of Double-Walled Boron Nitride Nano-Tubes (DWBNNTs) embedded in bundle of Carbon Nano-Tubes (CNTs) using nonlocal piezoelasticity cylindrical shell theory. In addition, Ghorbanpour Arani et al. [4] studied about nonlocal vibration of SWBNNT under a moving nano-particle. The effects of electric field, elastic medium, slenderness ratio and small scale parameter were investigated on the vibration behavior of SWBNNT under a moving nanoparticle. Results indicated the importance of using surrounding elastic medium in decrease of normalized dynamic deflection.

On the other hand, no report has studied the modeling of BNNBs for nano-switches. Nano-switches are fundamental devices in NEMS such as nanoscale actuators, pressure sensors and moving valves. A typical NEMS switch includes two parallel conducting electrodes, one of them is fixed and the other is flexible.

Moveable electrode is adjusted by an electrical potential difference, which creates it between the two electrodes. Direct Current (DC) voltage between the two electrodes results in the deflection of deformable electrodes and a consequent change in the system capacitance. In addition, the intermolecular interaction force also acts on the moveable electrode, which is directly dependent on the gap between them. Counteracting the electrostatic gathering intermolecular forces is the elastic force, which wants to restore the moveable electrode to its original position.

So the equilibrium position of the moveable electrode is defined by balancing of the intermolecular, electrostatic and elastic forces. When the voltage increases beyond a critical value, the moveable electrode becomes unstable and collapses onto the fixed electrode, so the nano-switch is in the ON state. For this state, it has seen an inherent instability, known as pull-in phenomenon that has been first observed experimentally [5-6]. The voltage and deflection of the switch at this state are called the pull-in displacement and pull-in voltage, respectively. An applied Alternating Current (AC) causes harmonic motions of the system, and resonant applications are obtained [6-14].

In addition, the reduction of the separation between the components of the switch will require the NEMS designs to account for intermolecular forces. In this case, the Casimir force has been considered. There is a specific distance for separation gap, ($g_0 \geq 1$ μm), that the moveable electrode is affected by this force.

The Casimir effect on the pull-in gap and pull-in voltage of NEMS switches was studied in [15-16]. Other works on nanoscale surface forces, such as the Casimir force were studied in [17-20]. Casimir force can be connected with the existence of zero-point vacuum oscillations of the electromagnetic field [18-20]. By using quantum field theory, these forces are formulated in [17-18]. It is determined that the Casimir force is more effective at larger separation distances between the components than the other intermolecular forces, like van der Waals force [17-20]. A distributed parameter model was studied by Ramezani et al. [21] to derive the pull-in instability of cantilever nano-mechanicall systems. The Casimir force between the electrodes is inversely proportional to the fourth power of the gap.

Yang et al. [22] discussed the pull-in instability of nano-switches under an electrostatic force and intermolecular Casimir force within nonlocal elasticity theory to account for the small scale effect. These studies are limited only to geometrically linear equations. Xiao et al. [23] studied pull-in instability of geometrically nonlinear micro-switches subjected to an electrostatic and Casimir forces. Although, this study has considered the geometrically nonlinear but it is about MEMS without any items of nanoscale. Also, Batra and his coworkers [24-25] considered von Karman geometric nonlinearity and Casimir force and developed the Reduced-Order Models (ROM) for the pull-in instability of the electrostatically actuated clamped rectangular, circular, and elliptic micro-plates, respectively. For a wide class of electrostatic NEMS bases, the deformable electrode is initially a flat body whose thickness, h, is much smaller than its characteristic in-plane dimension [26].

None of the above mentioned studies have considered the nonlinear higher order terms of strains and coupling effect of electro-mechanical relation based on the charge equation and nonlocal elasticity model presented by Eringen [27], which can enhance the accuracy of the results.

However, to date, no report has been found in the literature on the nonlinear pull-in voltage and deflection of BNNBs under intermolecular interaction force, and especially Casimir force. Herein, it is aimed to provide the nonlinear and nonlocal pull-in instability of BNNBs under direct voltage and combined forces. The higher order nonlinear governing equations are derived based on principle of virtual work and DQM is presented to demonstrate the effects of small scale parameter, electric potential and combined forces on pull-in phenomenon of the BNNBs which are discussed in details. In order to validate of this study, the linear equation is solved by MAD to evaluate the results with DQM and those obtained by Xiao et al. [23].

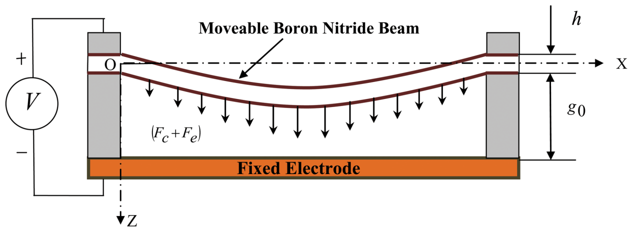

Figure 1. Configuration of BNNT under the combined electrostatic and Casimir force for nano-switch.

2. Mathematical model

Figure 1 depicts the structure of a typical nano-switch where the components are a fixed electrode as a ground plane and a moveable electrode as a BNNB of length L, width b and thickness h. It is separated by a dielectric spacer with an initial gap, g_0. V denotes the applied voltage (DC), so the beam deflects towards the fixed electrode under action of distributed electrostatic force, F_e, and intermolecular Casimir force, F_c.

2.1. Piezoelasticity EBB

In order to express the equation of equilibrium in the terms of mechanical and electrical components of displacement, the stress-strain relation for piezoelectric materials is given by [28]:

$$\{\sigma\} = [C]\{\varepsilon\} - [h]^T\{E\},$$
$$\{D\} = [h]\{\varepsilon\} + [\in]\{E\}, \tag{1}$$

where $\{\sigma\}$, $\{\varepsilon\}$, $\{E\}$ and $\{D\}$ are classical stress, strain, electric field tensor and Electric displacement tensor, respectively. Likewise $[C]$, $[h]$ and $[\in]$ denote elastic stiffness, piezoelectric and dielectric constants, respectively. In beam theory, stress-strain relation for piezoelectric materials under electro axial loading is given as:

$$\sigma_{xx} = E(\varepsilon_{xx}) - h_{11}E_x. \tag{2}$$

Electric displacement relation based on piezoelasticity theory can be expressed as:

$$D_x = h_{11}(\varepsilon_{xx}) + \in_{11} E_x, \tag{3a}$$

where $\in_{11}$ is the dielectric constant and E_x is given as [28]:

$$E_x = -\frac{\partial \phi}{\partial x}, \tag{3b}$$

where ϕ is electric potential. The effect of electric potential is seen in x-direction and ϕ must satisfy the electric boundary conditions like displacement components. According to Ke et al. [29], the electric potential can be assumed as a linear distribution of the electric potential in the thickness direction of the piezoelectric nano-beams. In this assumption, although there is an external electric voltage which can be generated by deflection and deformation, this external voltage is completely different from pull-in voltage and has no effect on the amount of pull-in voltage. To date, this type of voltage is being applied to smart control structures as sensors.

2.2. Strain-displacement relations

Based on EBB theory, the displacement field ($\tilde{U}$, $\tilde{W}$) of an arbitrary point on the moveable nano-beam can be expressed as [4]:

$$\tilde{U}(x,z) = -z\frac{\partial W(x)}{\partial x}, \tag{4}$$

$$\tilde{W}(x,z) = W(x), \tag{5}$$

where $W(x)$ is the transverse displacements of the point on the mid-plane (i.e., $Z = 0$). Using Eqs. (4) and (5), the strain-displacement relation can be written by von Karman-type nonlinear strain as:

$$\varepsilon_{xx} = -z\frac{\partial^2 W}{\partial x^2} + \frac{1}{2}\left(\frac{\partial W}{\partial x}\right)^2,$$
$$\gamma_{xz} = 0,$$
$$\varepsilon_{zz} = 0. \tag{6}$$

2.3. Nonlocal elasticity theory

Based on the nonlocal elasticity theory, the stress tensor at a reference point depends not only on the strain components at same position but also on all other points of the body. According to nonlocal elasticity theory, the basic equations for an isotropic linear homogenous nonlocal elastic body neglecting the body force are given as [27]:

$$\sigma_{ij,j} = 0,$$
$$\sigma_{ij}(X) = \int_V \phi\left(\left|\vec{X} - \vec{X'}\right|, \alpha\right) t_{ij} dV\left(\vec{X'}\right), \quad \forall \vec{X} \in V,$$
$$t_{ij} = \xi_{ijkl}\varepsilon_{kl},$$
$$\varepsilon_{ij} = \frac{1}{2}(u_{i,j} + u_{j,i}). \tag{7}$$

The terms σ_{ij}, t_{ij}, ε_{ij} and ξ_{ijkl} are the nonlocal stress, classical stress, classical strain and fourth order elasticity tensors, respectively. The volume integral is over the region V occupied by the body. Eq. (1) represents the relations between nonlocal and classical stresses based on Eringen's nonlocal continuum theory in which the kernel function $\phi(\vec{X} - \vec{X'}|, \alpha)$ is the nonlocal modulus. The nonlocal modulus acts as an attenuation function incorporating into constitutive equations where the nonlocal effects at the reference point (i.e. $\vec{X}$) can be produced by local strain at the source (i.e. $\vec{X'}$). The term $|\vec{X}-\vec{X'}|$ represents the distance in the Euclidean form and α is a material constant that depends on the internal (e.g. lattice parameter, granular size and distance between the C-C bonds) and external characteristics lengths (e.g. crack length and wave length). Material constant α is defined as [27]:

$$\alpha = \frac{e_0 a}{l}, \tag{8}$$

where e_0 is a constant appropriate to each material. The parameter e_0 was given as 0.39 which has to be determined from experiments by matching dispersion curves of plane waves. Also, parameter a shows internal characteristic length, and it was chosen as the length of C-C bond, which is 0.142 nm. The term l is the external characteristic length of the nanostructure. The nonlocal constitutive stress-strain relation at small scale can be simplified as:

$$(1-\alpha^2 l^2 \nabla^2)\sigma_{ij} = t_{ij}, \tag{9}$$

where ∇^2 is the Laplacian. The above nonlocal constitutive equation (Eq. (9)) has been recently used widely for the study of micro- and nano-structure elements. Therefore, Eqs. (2) and (3a) in nonlocal form can ber written as follows [27]:

$$\left(1-(e_0 a)^2\nabla^2\right)\sigma_{xx} = E(\varepsilon_{xx}) - h_{11}E_x, \tag{10}$$

$$\left(1-(e_0 a)^2\nabla^2\right)D_x = h_{11}(\varepsilon_{xx}) + \in_{11} E_x. \tag{11}$$

2.4. Electrostatic force

From an electrical point of view, the system behaves as a variable gap capacitor. By assuming that $\frac{g_0}{L} << 1$, the value F_e of the electrostatic force acting on the deformable electrode is given by [30]:

$$F_e = \frac{\varepsilon_0 b V^2}{2(g_0-W)^2}\left(1+0.65\frac{(g_0-W)}{b}\right), \tag{12}$$

in which $\varepsilon_0 = 8.854 \times 10^{-12}$ $C^2N^{-1}m^{-2}$ is the permittivity of vacuum. Therefore, the expression for the electrostatic force depends only on the gap (g_0). Also, for small strains and moderate rotations involved, F_e is assumed to act along the normal to the fixed beam. It should be noted that the second term of Eq. (10), $0.65\frac{\varepsilon_0 V^2}{2(g_0-W)}$, is the fringing field force. Based on Ghorbanpour et al. [31], fringing field force has a great effect on the pull-in phenomenon. The pull-in voltage increases when the fringing field is eliminated from equations, and so, switches need higher voltage to pull-in on the ground plane.

2.5. Intermolecular force

The Casimir force between two surfaces depends on the dielectric properties of the surfaces and also on the geometric parameters [32,33]. The Casimir force per unit length of the actuator is [34]:

$$F_c = \frac{\pi^2 \bar{h} c b}{240(g_0-W)^4}, \tag{13}$$

where $\bar{h} = 1.055 \times 10^{-34} Jc$ is the reduced Planck's constant and $c = 2.998 \times 10^8$ $\frac{\text{m}}{\text{s}}$ is the speed of light. When actuators are wider enough than the separation distance, Eq. (13) can provide acceptable results [32]. In this study, the nano-actuators that are wider than the separation distance ($\frac{g_0}{w} < 1$) are considered. For separation distances larger than 1 μm, the interaction between the bodies is described only by the Casimir force, (see Eq. (12)). Consequently, at large separation distances the interaction force is independent of the material properties of bodies.

Regarding Eqs. (12) and (13), it should be stated that when an electrical potential difference is created between the two electrodes, the induced electrostatic charge gives rise to electrostatic force which deflects the moveable electrode towards the fixed electrode. In addition, the intermolecular interaction force which is directly dependent on the gap between them also acts on the moveable electrode, altering its deflection. Counteracting the electrostatic and intermolecular forces is the elastic force, which tries to restore the moveable electrode to its original position. With continuing reduction in the size, the surface traction due to molecular interaction between two surfaces plays an important role in the deflection of micro-switches and can be described by the Casimir force or the van der Waals force, depending on the gap between the electrodes [17,35]. When the gap is less than 20 nm, in this case, the intermolecular force between two surfaces is estimated as the vdW attraction and varies as the inverse cube of the separation and is affected by material properties [34]. For separations large enough (such as above 20 nm), the intermolecular force between two surfaces can be described by the Casimir interaction which is proportional to the inverse fourth power of the separation and it is not affected by material properties [17].

3. Governing equation

The total potential energy, V, of nano-switch is the sum of strain energy, U and W_c, W_e as external works for Casimir force, and electrostatic force, respectively, which is expressed as:

$$V = U - W_c - W_e. \tag{14}$$

The strain energy of BNNB can be written as:

$$U = \frac{1}{2}\int_0^L \int_A (\varepsilon_{xx} - E_x)\begin{Bmatrix}\sigma_{xx}\\ D_x\end{Bmatrix} dAdx, \tag{15}$$

using the resultant forces and moments in the middle surface of BNNB which are defined as:

$$N_x = \int_A \sigma_{xx} dA, \tag{16}$$

$$M_x = \int_A \sigma_{xx} z dA. \tag{17}$$

The total strain energy can be written as:

$$U_s = \frac{1}{2}\int_0^L \left[\left(-M_x \frac{\partial^2 W}{\partial x^2} + \frac{1}{2}N_x\left(\frac{\partial W}{\partial x}\right)^2\right) - \left(\int_A \left(D_x\left(-\frac{\partial \phi}{\partial x}\right)\right) dA\right)\right] dx. \tag{18}$$

The external work due to intermolecular forces and electrostatic force are written as:

$$W_v = \frac{1}{2}\int_0^L (F_c + F_e) W dx = \frac{1}{2}\int_0^L \left(\frac{\pi^2 \bar{h} cb}{240(g_0 - W)^4} + \frac{\varepsilon_0 b V^2}{2(g_0 - W)^2}\left(1 + 0.65\frac{(g_0 - W)}{b}\right)\right) W dx. \tag{19}$$

By employing the principle of virtual work ($\delta(U_s - W_v) = 0$) and setting the coefficient of mechanical and electrical to zero, the governing differential equilibrium equations are derived as:

δW:

$$\left(-\frac{\partial^2 M_x}{\partial x^2}\right) + \left(\frac{\partial N_e}{\partial x}\right)\left(\frac{\partial W}{\partial x}\right) + N_e \frac{\partial^2 W}{\partial x^2} - (F_c + F_e) = 0, \tag{20}$$

$\delta \phi$:

$$\frac{\partial D_x}{\partial x} = 0, \tag{21}$$

where $N_e = -h_{11} A \frac{\partial \phi}{\partial x}$ is electrical force. Using Eqs. (3), (5), (10) and (11), Eqs. (15) and (16) can be expanded as:

$$M_x - (e_0 a)^2 \frac{\partial^2 M_x}{\partial x^2} = -EI\frac{\partial^2 W}{\partial x^2}, \tag{22}$$

$$D_x - (e_0 a)^2 \nabla^2 D_x = h_{11}\left(-z\frac{\partial^2 W}{\partial x^2} + \frac{1}{2}\left(\frac{\partial W}{\partial x}\right)^2\right) + \in_{11}\left(-\frac{\partial \phi}{\partial x}\right). \tag{23}$$

Using Eringen's nonlocal elasticity model and Eqs. (22) and (23), the motion equations (i.e. Eqs. (20) and (21)) can be drived as:

$$\begin{aligned}&\left(EI\frac{\partial^4 W}{\partial x^4}\right) - h_{11}A\left(\frac{\partial^2 \phi}{\partial x^2}\right)\left(\frac{\partial W}{\partial x}\right) - h_{11}A\frac{\partial \phi}{\partial x}\left(\frac{\partial^2 W}{\partial x^2}\right) = \frac{\pi^2 \bar{h} cb}{240}\left(\frac{1}{(g_0 - W)^4} - (e_0 a)^2 \frac{41}{(g_0 - W)^5}\left(\frac{\partial^2 W}{\partial x^2}\right) - (e_0 a)^2 \frac{20}{(g_0 - W)^6}\left(\frac{\partial W}{\partial x}\right)^2\right)\\ &+ \left(\frac{\varepsilon_0 b V^2}{2}\left(\frac{1}{(g_0 - W)^2} + \frac{0.65}{b(g_0 - W)} - (e_0 a)^2\left(\frac{2}{(g_0 - W)^3} + \frac{0.65}{(g_0 - W)^2}\right)\left(\frac{\partial^2 W}{\partial x^2}\right) - (e_0 a)^2\left(\frac{6}{(g_0 - W)^4} + \frac{1.3}{(g_0 - W)^3}\right)\times\left(\frac{\partial W}{\partial x}\right)^2\right),\end{aligned} \tag{24}$$

$$h_{11}\left(\frac{\partial W}{\partial x}\right)\left(\frac{\partial^2 W}{\partial x^2}\right) - \in_{11}\left(\frac{\partial^2 \phi}{\partial x^2}\right) = 0. \tag{25}$$

After that, we can define dimensionless parameters as:

$$\begin{aligned}&\bar{w} = \frac{W}{g}, && \mu = \frac{(e_0 a)}{L},\\ &\beta = \frac{\varepsilon_0 b V^2 L^4}{2 g_0^3 EI}, && \lambda = \frac{\bar{A} b L^4}{6\pi EI g_0^4},\\ &\bar{x} = \frac{x}{L}, && \bar{\phi} = \frac{h_{11} L}{AEI}\phi,\\ &\zeta = \frac{A g_0^2}{I}, && \gamma = \frac{\in_{11} EI}{A h_{11}^2 g_0^2},\\ &f = 0.65\frac{g_0}{b}.\end{aligned} \tag{26}$$

By substituting Eq. (26) into Eqs. (24) and (25), the dimensionless equilibrium equations can be rewritten as:

$$\left(\frac{\partial^4\bar{w}}{\partial\bar{x}^4}\right)-\left(\frac{\partial^2\bar{\phi}}{\partial\bar{x}^2}\right)\left(\frac{\partial\bar{w}}{\partial\bar{x}}\right)-\left(\frac{\partial\bar{\phi}}{\partial\bar{x}}\right)\left(\frac{\partial^2\bar{w}}{\partial\bar{x}^2}\right)$$
$$=\left(f\beta\frac{1}{(1-\bar{w})}+\beta\frac{1}{(1-\bar{w})^2}+R_c\frac{1}{(1-\bar{w})^4}\right)$$
$$-\left(f\beta\mu^2\frac{1}{(1-\bar{w})^2}+2\beta\mu^2\frac{1}{(1-\bar{w})^3}\right.$$
$$\left.+4R_c\mu^2\frac{1}{(1-\bar{w})^5}\right)\left(\frac{\partial^2\bar{w}}{\partial\bar{x}^2}\right)$$
$$-\left(2f\beta\mu^2\frac{1}{(1-\bar{w})^3}+6\beta\mu^2\frac{1}{(1-\bar{w})^4}\right.$$
$$\left.+20R_c\mu^2\frac{1}{(1-\bar{w})^6}\right)\left(\frac{\partial\bar{w}}{\partial\bar{x}}\right)^2\Bigg), \tag{27}$$

$$\left(\frac{\partial\bar{w}}{\partial\bar{x}}\right)\left(\frac{\partial^2\bar{w}}{\partial\bar{x}^2}\right)-\gamma\left(\frac{\partial^2\bar{\phi}}{\partial\bar{x}^2}\right)=0. \tag{28}$$

Three different boundary conditions of the moveable electrode are considered in the present analysis and the above equations are solved by the boundary conditions:

Clamped-Clamped:

$$\text{at}\quad \bar{x}=0,1\qquad \bar{w}=0,\quad \frac{\partial\bar{w}}{\partial\bar{x}}=0. \tag{29a}$$

Clamped-Simply:

$$\text{at}\quad \bar{x}=0\qquad \bar{w}=0,\quad \frac{\partial\bar{w}}{\partial\bar{x}}=0,$$

$$\text{at}\quad \bar{x}=1\qquad M_x=0\Rightarrow\frac{\partial^2\bar{w}}{\partial\bar{x}^2}=0. \tag{29b}$$

Simply-Simply:

$$\text{at}\quad \bar{x}=0,1\qquad \bar{w}=0,\quad M_x=0\Rightarrow\frac{\partial^2\bar{w}}{\partial\bar{x}^2}=0. \tag{29c}$$

4. Solution method and numerical results

No published report has been found in the literature against which the output of this paper could be validated. So, we used two different numerical methods (DQM and MAD) to solve the equations and validate the figures and results.

4.1. DQM

In this method, the partial derivative of a function with respect to spatial variables at a given discrete point is approximated as a weighted linear sum of the function values at all discrete points chosen in the solution domain. According to this method, the functions $\bar{w}$, $\bar{\phi}$ and their derivatives are approximated as [36-38]:

$$\frac{d^k}{d\bar{x}^k}\{\bar{w},\bar{\phi}\}\big|_{\bar{x}=\bar{x}_n}=\sum_{m=1}^{N}C_{nm}^{(k)}\{\bar{w}_m,\bar{\phi}_m\}, \tag{30}$$

where N is the grid points along $\bar{x}$ and C_{nm} represent the Lagrange interpolation polynomial as:

$$C_{nm}^{1}=\frac{\pi(\bar{x}_n)}{(\bar{x}_n-\bar{x}_m)\pi(\bar{x}_m)},$$
$$n,m=1,2,\cdots,N;\qquad n\neq m, \tag{31a}$$

where $\pi(\bar{x}_n)$ in the above equation is defined as:

$$\pi(\bar{x}_n)=\prod_{m=1}^{N}(\bar{x}_n-\bar{x}_m),\qquad n\neq m,$$

$$C_{nm}^{(1)}=C_{mm}^{(1)}=-\sum_{t=1}^{N}C_{nm}^{(1)},$$

$$n=1,2,\cdots,N;\qquad n\neq m, \tag{31b}$$

where C_{nm} represents the weighting coefficients. The weighting coefficients for the high order derivatives are determined via matrix multiplication.

$$C_{nm}^{(2)}=\sum_{t=1}^{N}C_{nt}^{(1)}C_{tm}^{(1)},\qquad C_{nm}^{(3)}=\sum_{t=1}^{N}C_{nt}^{(1)}C_{tm}^{(2)},$$

$$C_{nm}^{(4)}=\sum_{t=1}^{N}C_{nt}^{(1)}C_{tm}^{(3)}. \tag{31c}$$

Applying DQM approximations to the governing equations (Eqs. (27) and (28)) we obtain:

$$\sum_{t=1}^{N}C_{nm}^{(4)}\bar{w}_m-\sum_{t=1}^{N}C_{nm}^{(2)}\bar{\phi}_m\sum_{t=1}^{N}C_{nm}^{(1)}\bar{w}_m$$
$$-\sum_{t=1}^{N}C_{nm}^{(1)}\bar{\phi}_m\sum_{t=1}^{N}C_{nm}^{(2)}\bar{w}_m=q_{1i}+q_{2i}\sum_{t=1}^{N}C_{nm}^{(2)}\bar{w}_m$$
$$+q_{3i}\left(\sum_{t=1}^{N}C_{nm}^{(1)}\bar{w}_m\right)^2, \tag{32a}$$

$$\sum_{t=1}^{N}C_{nm}^{(1)}\bar{w}_m\sum_{t=1}^{N}C_{nm}^{(2)}\bar{w}_m-\gamma\sum_{t=1}^{N}C_{nm}^{(2)}\bar{\phi}_m=0, \tag{32b}$$

where q_{1i}, q_{2i} and q_{3i} are defined as:

$$q_{1i}=+\left(f\beta\frac{1}{(1-\bar{w}_i)}+\beta\frac{1}{(1-\bar{w}_i)^2}+R_c\frac{1}{(1-\bar{w}_i)^4}\right), \tag{33a}$$

$$q_{2i}=-\left(f\beta\mu^2\frac{1}{(1-\bar{w}_i)^2}+2\beta\mu^2\frac{1}{(1-\bar{w}_i)^3}+4R_c\mu^2\frac{1}{(1-\bar{w}_i)^5}\right)\left(\frac{\partial^2\bar{w}_i}{\partial\bar{x}^2}\right), \tag{33b}$$

$$q_{3i}=-\left(2f\beta\mu^2\frac{1}{(1-\bar{w}_i)^3}+6\beta\mu^2\frac{1}{(1-\bar{w}_i)^4}+20R_c\mu^2\frac{1}{(1-\bar{w}_i)^6}\right)\left(\frac{\partial\bar{w}_i}{\partial\bar{x}}\right)^2. \tag{33c}$$

Accordingly, the boundary conditions become:

Clamped-Clamped:

$$\bar{x}=0 \qquad \bar{w}_1=0, \quad \sum_{t=1}^{N}C_{1m}^{(1)}\bar{w}_m=0,$$

$$\bar{x}=1 \qquad \bar{w}_N=0, \quad \sum_{t=1}^{N}C_{Nm}^{(1)}\bar{w}_m=0. \tag{34a}$$

Clamped-Simply:

$$\bar{x}=0 \qquad \bar{w}_1=0, \quad \sum_{t=1}^{N}C_{1m}^{(1)}\bar{w}_m=0,$$

$$\bar{x}=1 \qquad \bar{w}_N=0, \quad \sum_{t=1}^{N}C_{Nm}^{(2)}\bar{w}_m=0. \tag{34b}$$

Simply-Simply:

$$\bar{x}=0 \qquad \bar{w}_1=0, \quad \sum_{t=1}^{N}C_{1m}^{(2)}\bar{w}_m=0,$$

$$\bar{x}=0 \qquad \bar{w}_N=0, \quad \sum_{t=1}^{N}C_{Nm}^{(2)}\bar{w}_m=0, \tag{34c}$$

denoting the unknown static displacement and potential electric field vector by $X=\{\bar{w}_i^T,\bar{\phi}_i^T\}^T$ and the transverse linear and nonlinear force vector by $q_L=\{q_{Li}\}^T$, $q=\{q_i\}^T$, respectively. Voltage Iteration (VI) algorithm is used to obtain the linear and nonlinear solutions of pull-in parameters.

For solving Eqs. (32) and (33), we first reduce Eq. (32) to the geometric linearity equation. Then, by reducing the right hand side of Eq. (32) to the linear part via the Taylor series expansion ($q_L=\{q_{Li}\}^T$), the equations are solved by choosing a trial voltage, then increasing the trial voltage (V) and repeating the earlier steps, until $\bar{w}$ converges. So, the last trial voltage V, under which the deflection is solvable, is the linear pull-in voltage and the corresponding deflection is the linear pull-in deflection. This method is named Iteration Voltage (IV) and was used in [23] to obtain pull-in parameters. Afterward, the geometric nonlinearity answer is obtained by iteration from substituting the linear answer to the algebraic equation system.

$$\begin{bmatrix}K_{1w} & K_{1\phi}\\ K_{2w} & K_{2\phi}\end{bmatrix}\begin{bmatrix}\bar{w}_i\\ \bar{\phi}_i\end{bmatrix}=\begin{bmatrix}q_i\\ 0\end{bmatrix}. \tag{35}$$

The above steps are repeated to obtain the nonlinear pull-in parameters. The last trial voltage V under which the deflection is convergent is the nonlinear pull-in voltage V_{PI}.

4.2. Numerical results and discussion

The results are based on the following data used for the geometric and material properties of BNNBs. Geometry and constitutive material of the beams are showed in Table 1 [4,21,23]. In the following subsections, the effects of small scale, length of beam changes, electric potential, Casimir force, pull-in voltage and separation gap BNNBs are studied and discussed in details.

Plotted in Figure 2 are curves showing the effect of small scale effect (μ) on the maximum deflection versus applied voltage V that it was derived from the answer

Table 1. Geometric and material parameters of nano-beam (BNNB).

b (μm)	h (μm)	g_0 (μm)	E (Tpa)	$\in_{11}$ (c/m)	e_0a (nm)
100	1.5	1	1.8	0.95	0.118572

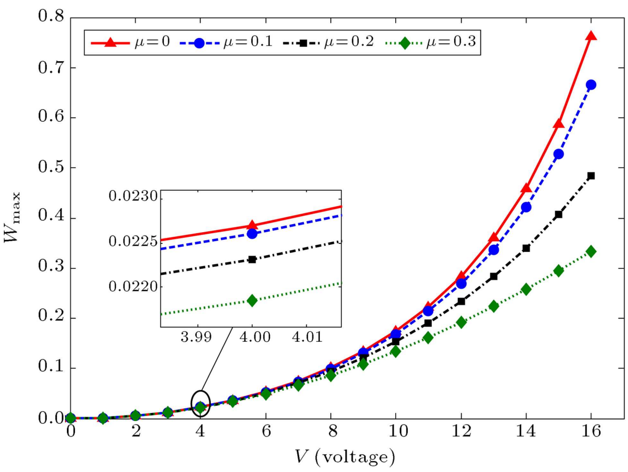

Figure 2. Effects of nonlocal parameter on deflection.

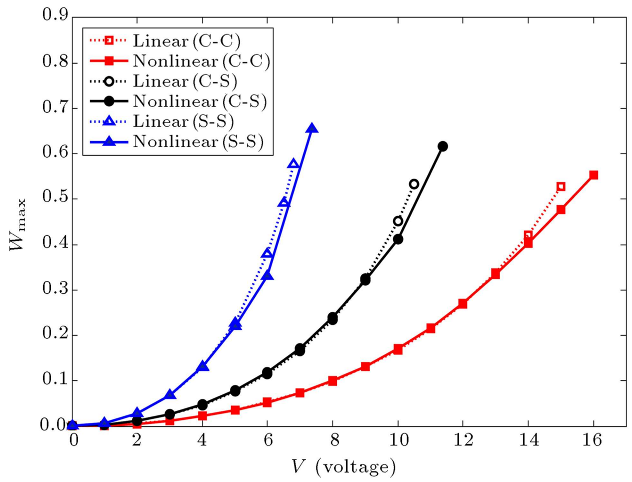

Figure 3. Variation of the boundary conditions on applied voltage V with the maximum deflection.

of nonlinear equations. As can be seen, considering small scale effect decreases the deflection of BNNBs especially under higher voltages.

Figure 3 illustrates the relationship between applied voltage V and the maximum deflection $\bar{w}_{\max}$ of the nano-beams with ($\mu = 0.1$). As expected, the C-C nano-beam has considerably higher pull-in voltage than the other two types while the C-S nano-beam has the lower pull-in voltage and the lowest pull-in voltage belongs the S-S boundary condition. Before pull-in condition, the nonlinear deflection is smaller than the linear ones at the same applied voltage. The pull-in voltage and deflection are obtained from the nonlinear analysis, however, are larger than those calculated from the linear analysis.

Table 2 presents the convergence study of the present analysis by comparing the pull-in voltages of S-S nano-beams of different length with varying total number of sampling points N. Material properties are given in Table 1. For selected values of (μ), the pull-in voltages of the switch can be extracted from Table 3 for $L = 310$ μm.

The pull-in voltage V_{PI} with varying gap g_0 is given in Figure 4. It is noted that with an increase in gap values, the calculated pull-in voltage V_{PI} from both the nonlinear and the linear analysis increases.

Figure 5 indicates the maximum deflection $\bar{w}_{\max}$ versus pull-in voltage of C-C BNNB with varying

Table 3. Pull-in voltage of S-S BN nano-beams with varying (μ).

$L = 310$ (μm)		$\mu = 0$	$\mu = 0.2$	$\mu = 0.3$
$N = 13$	Linear	17.29	19.03	22.18
	Non-linear	19.95	19.63	22.78
$N = 17$	Linear	17.29	19.03	22.18
	Non-linear	19.95	19.63	22.78

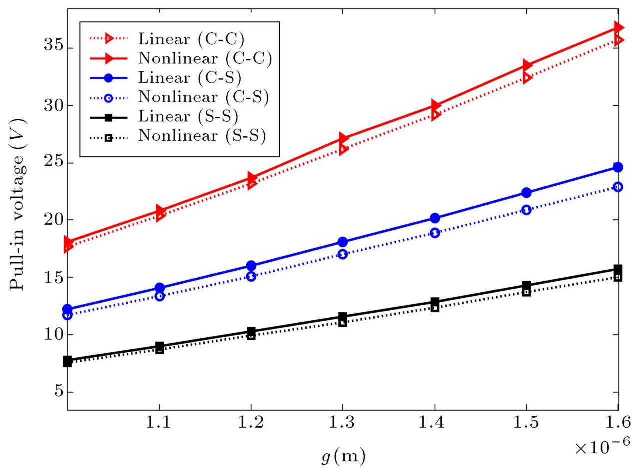

Figure 4. Variation of BNNT pull-in voltage with various gap (g_0).

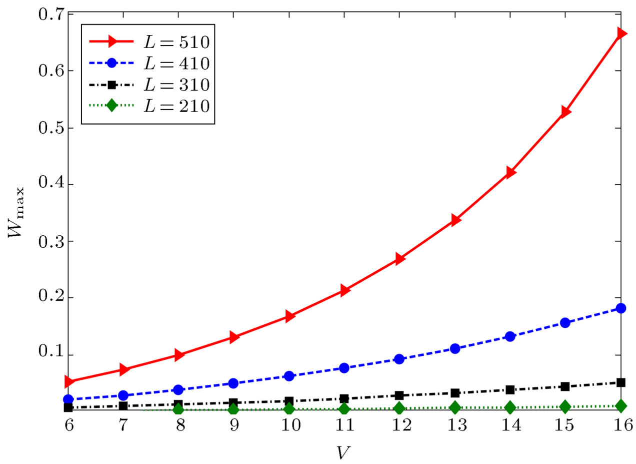

Figure 5. Maximum deflection against length of BN (C-C) nano-beam.

Table 2. Pull-in voltage of S-S BN nano-beams with ($\mu = 0.1$).

L (μm)	$N = 7$		$N = 11$		$N = 15$	
	Linear	Non-linear	Linear	Non-linear	Linear	Non-linear
510	6.53	7.25	6.53	7.25	6.53	7.25
410	10.11	11.24	10.11	11.24	10.11	11.24
310	17.68	19.66	17.68	19.66	17.68	19.66
210	38.53	44.67	38.53	44.67	38.53	44.67

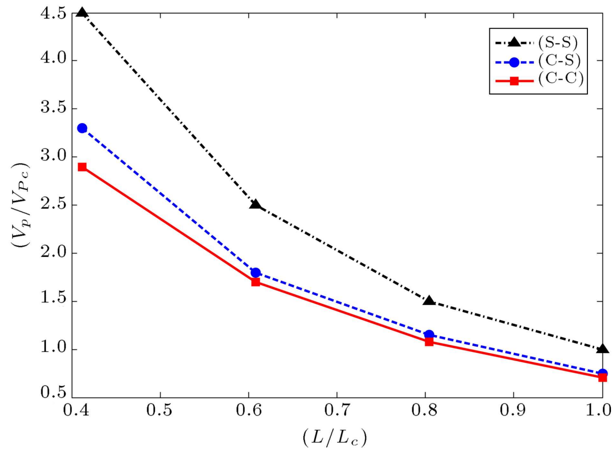

Figure 6. Dimensionless pull-in voltage versus dimensionless beam length ($L_c = 510$) for three boundary conditions.

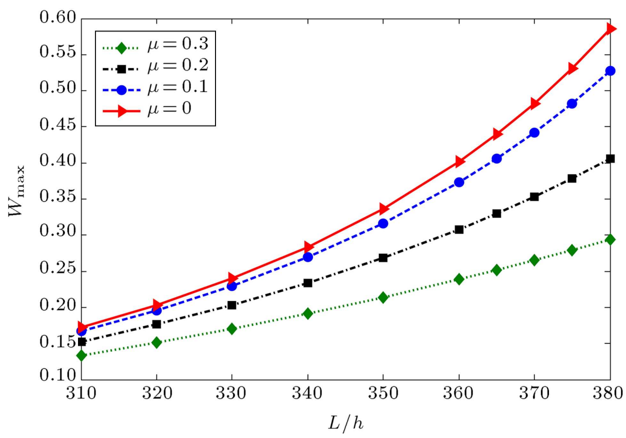

Figure 7. Maximum deflection with various lengths to thickness ratio with different values of small scale.

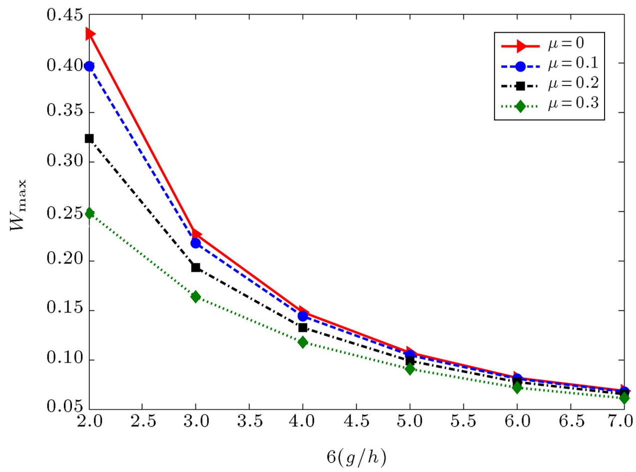

Figure 8. Maximum deflection with various $6(\frac{g}{h})^2$ ratios with different values of small scale.

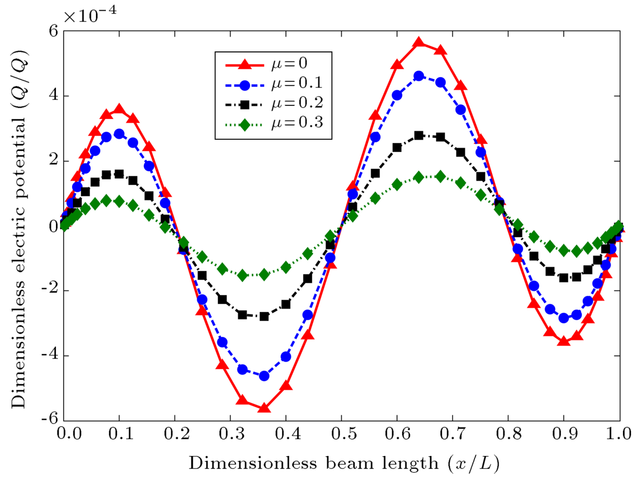

Figure 9. Variation of non-dimensional of electric potential along the (C-C) nanobeam with different values of small scale.

length. It can be seen that the pull-in voltage decreases with an increase in length magnitudes of beam, which indicates that the nano-beam with a lower length can sustain a higher voltage. The results for nano-beams under other two boundary conditions are compared in Figure 6. The effect of boundary conditions on the pull-in voltage versus non-dimensional beam length is demonstrated in Figure 6. The results indicate that increasing the non-dimensional beam length decreases pull-in voltage. As expected, the C-C nano-beam is more stable than the other types of boundary conditions.

The effects of small scale effect (μ) on the pull-in voltage V_{PI} versus length ratio (L/h) for $V = 12$ is shown in Figure 7. It is noted that with an increase in length ratio, the pull-in voltage V_{PI} decreases. Also, increase in the value of small scale effect lead to a decrease in the maximum deflection.

Figure 8 represents the maximum deflection ($\bar{w}_{\max}$) versus various $6(\frac{g}{h})^2$ ratio for different values of small scale. In realizing the influence of the small scale effect, Figure 8 shows how the dimensionless maximum deflection changes with respect to the dimensionless $6(\frac{g}{h})^2$ ratio. It is found from Figure 8 that $\bar{w}_{\max}$ for the BNNB decreases with increase of small scale parameter. Figure 9 shows distribution of electric potential ϕ for all grid points, which located on beam length with different values μ. It is clear that electric potential at boundary conditions is constant and equal to zero in which its curves is changed with variation of μ. It is remarkable that with an increase in μ, changes in the electric potential decrease, too. This is because the electric potential is directly proportional to deflection.

As can be seen from Figure 10, increasing of the small scale parameters shifts curves down. However, according to specific characteristic of piezoelectric, any increase in the value of μ leads to an increase in the pull-in voltage. Also, the magnitudes of voltage have direct proportion with electric potential.

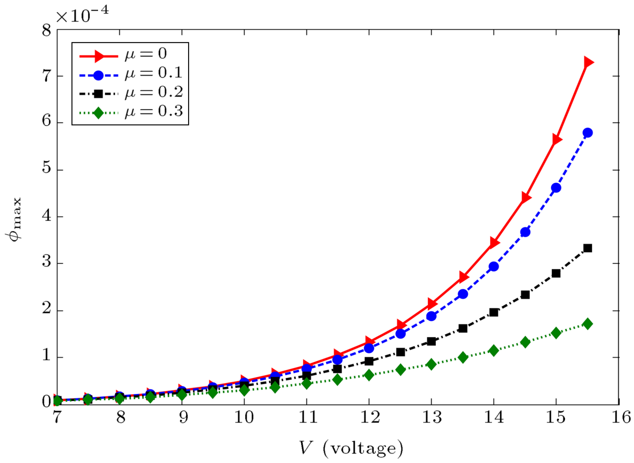

Figure 10. Effect of nonlocal parameter on non-dimensional electric potential with various voltages.

4.3. MAD

For solving Eq. (27) by MAD and reducing it to the common form, it is convenient to rewrite Eq. (27) as:

$$\left(\frac{\partial^4\bar{w}}{\partial\bar{x}^4}\right)=\left(f\beta\frac{1}{(1-\bar{w})}+\beta\frac{1}{(1-\bar{w})^2}+R_c\frac{1}{(1-\bar{w})^4}\right). \quad (36)$$

Noted that the above equation is linear form of Eq. (27).

Clamped-Clamped:

$$\text{in} \quad \bar{x}=0: \qquad \bar{w}=0, \quad \bar{w}'=0,$$

$$\text{in} \quad \bar{x}=1: \qquad \bar{w}=0, \quad \bar{w}'=0, \quad (37)$$

the solution process of Eq. (36) becomes:

$$\left(\frac{\partial^4\bar{w}}{\partial\bar{x}^4}\right)=\left(\frac{A}{(1-\bar{w})}+\frac{B}{(1-\bar{w})^2}+\frac{D}{(1-\bar{w})^4}\right):$$

$$A=f\beta, \qquad B=\beta, \qquad C=R_c. \quad (38)$$

The deflection of BNNBs in Eq. (36) can be represented as [37-41]:

$$\bar{w}(x)=\sum\bar{w}_n=\bar{w}(0)+A'x+B'\frac{x^2}{2}+C'\frac{x^3}{3!}+L^{-1}\left(\sum f_A\right)+L^{-1}\left(\sum f_B\right)+L^{-1}\left(\sum f_D\right), \quad (39)$$

where $f_A=\frac{A}{1-\bar{w}}$, $f_B=\frac{B}{(1-\bar{w})^3}$, $f_D=\frac{D}{(1-\bar{w})^4}$ and the constants A', B' and C' can be determined by boundary conditions. Also L^{-1} is an inverse operator which is considered a fourfold integral operator defined by:

$$L^{-1}(.)=\int_0^x\int_0^x\int_0^x\int_0^x(.)dxdxdxdx. \quad (40)$$

Based on this identification, the method formally admits the use of the recursive relation:

$$\left[\begin{aligned}&\bar{w}_0(x)=0,\\&\bar{w}_1(x)=A'x+B'\frac{x^2}{2}+C'\frac{x^3}{3!}+L^{-1}\left(\sum f_{A_0}\right)+L^{-1}\left(\sum f_{B_0}\right)+L^{-1}\left(\sum f_{D_0}\right),\\&\bar{w}_{k+1}(x)=L^{-1}\left(\sum f_{A_k}\right)+L^{-1}\left(\sum f_{B_k}\right)+L^{-1}\left(\sum f_{D_k}\right), \qquad k\rangle 0,\end{aligned}\right. \quad (41)$$

for the determination of the components $\bar{w}_k(x)$ of $\bar{w}(x)$. Applying the above data for the Fixed_Fixed switch, and applying Eqs. (36)-(41) to the equations in Appendix A results in the governing equations:

$$\bar{w}(x)=\bar{w}_0+\bar{w}_1+\bar{w}_2, \quad (42)$$

$$\bar{w}(x)=0+\left(\frac{B'}{2!}x^2+\frac{C'}{3!}x^3+\frac{(f\times\beta+\beta+R_c)}{4!}x^4\right)+(f\times\beta+2\beta+4R_c)\times\left(\frac{B'}{6!}x^6+\frac{C'}{7!}x^7+\frac{(f\times\beta+\beta+R_c)}{8!}x^8\right). \quad (43)$$

The constants A', B' and C' can be determined by solving the resulted algebraic equation from the boundary condition at $\bar{x}=1$. 55 The answer obtained by MAD is compared with DQM's answer of linear motion equation (i.e. Eq. (35)) and nonlinear one (i.e. Eqs. (27)) for clamped-clamped boundary condition in Figure 11.

Figure 11 illustrates curves showing a simple comparison between DQM's answers of BNNB and the answer of the MAD method for Eq. (36). In the lower voltage, the difference between answers of those methods is little and is more precise.

To date, no experimental results have been published in the literature on the Boron Nitride nano-switches but it is possible to compare our numerical results with the published papers in this field. Figure 12 shows comparison of the present results with those reported by Xiao et al. [23]. In mentioned study, the authors worked on nonlinear analysis of micro-switches modeled by EBB. In that study, the deflection equation was solved by DQM in which there was a comparison

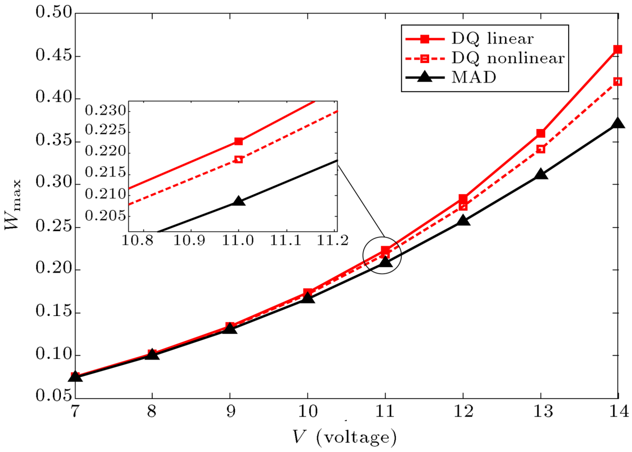

Figure 11. Comparison of pull-in parameters by two methods for (C-C) BNNB.

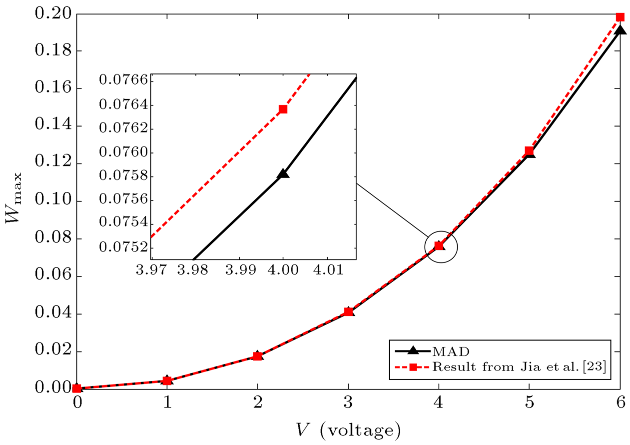

Figure 12. Comparison of maximum deflection between the present work and Xiao et al. [23].

between voltage and the maximum deflection. Now, their results have been compared with this work which is calculated by MAD method. Also, it is found from this figure that the obtained results from MAD for geometric linearity equation is more accurate in lower voltages.

5. Conclusions

The pull-in phenomenon of BNNBs using nonlocal piezoelasticity theory under electrostatic and Casimir force was investigated. The governing equations were solved numerically through DQM and MAD to obtain pull-in voltage. It could be realized that the comparison of pull-in voltage, with respect to nonlocal parameters, with electric potential, length of beam and gap were investigated. The major conclusions obtained are as follows:

1. Increase in the values of small scale parameter leads to increase in the pull-in voltage magnitude to reach the instability condition.
2. The clamped-clamped boundary condition has higher value of pull-in voltage.
3. Increasing the value of the gap leads to increase in the magnitude of the pull-in voltage.
4. It is observed that an increase in the value of small scale parameter causes to decrease the potential field in the length of the beam.
5. Comparing between MAD and DQM, it is found that in lower voltage values, the results have a good convergence.

Acknowledgments

The author would like to thank the reviewers for their comments and suggestions to improve the clarity of this article. The authors are grateful to University of Kashan for supporting this work by Grant No. 363443/1. They would also like to thank the Iranian Nanotechnology Development Committee for their financial support.

References

1. Ghorbanpour Arani, A., Amir, S., Shajari, A.R. and Mozdianfard, M.R. "Electro-thermo-mechanical buckling of DWBNNTs embedded in bundle of CNTs using nonlocal piezoelasticity cylindrical shell theory", *Composite Part B*, **43**, pp. 195-203 (2012).
2. Oh, E.S. "Elastic properties of boron-nitride nanotubes through the continuum lattice approach", *Materials Letters*, **64**, pp. 859-862 (2010).
3. Song, J., Huang, Y., Jiang, H., Hwang, K.C. and Yu, M.F. "Deformation and bifurcation analysis of boron-nitride nanotubes", *International Journal of Mechanical Science*, **48**, pp. 1197-1207 (2006).
4. Ghorbanpour Arani, A., Roudbari, M.A. and Amir, S. "Nonlocal vibration of SWBNNT embedded in bundle of CNTs under a moving nanoparticle", *Physica B*, **407**, pp. 3646-3653 (2012).
5. Taylor, G.I. "The coalescence of closely spaced drops when they are at different electric potentials", *Proceedings of the Royal Society A*, **306**, pp. 423-434 (1968).
6. Nathanson, H.C., Newell, W.E., Wickstrom, R.A. and Davis, J.R. "The resonant gate transistor", *IEEE Transactions on Electron Devices*, **14**, pp. 117-133 (1967).
7. Abdel-Rahman, E.M., Younis, M.I. and Nayfeh, A.H. "Characterization of the mechanical behavior of an electrically actuated microbeam", *Journal of Micromechanics and Microengineering*, **12**, pp. 759-766 (2002).
8. Kuang, J.H. and Chen, C.J. "Dynamic characteristics of shaped micro-actuators solved using the differential quadrature method", *Journal of Micromechanics and Microengineering*, **14**, pp. 647-655 (2004).

9. Krylov, S. and Maimon, R. "Pull-in dynamics of an elastic beam actuated by continuously distributed electrostatic force", *Journal of Vibration and Acoustics*, **126**, pp. 332-342 (2002).

10. Nayfeh, A.H. and Younis, M.I. "Dynamics of MEMS resonators under superharmonic and subharmonic excitations", *Journal of Micromechanics and Microengineering*, **15**, pp. 1840-1847 (2005).

11. Xie, W.C., Lee, H.P. and Lim, S.P. "Nonlinear dynamic analysis of MEMS switches by nonlinear modal analysis", *Nonlinear Dynamics*, **31**, pp. 243-256 (2003).

12. Tilmans, H.A. and Legtenberg, R. "Electrostatically driven vacuum-encapsulated polysilicon resonators: Part I. Design and Fabrication", *Sensors and Actuators A*, **45**, pp. 57-66 (1994).

13. Tilmans, H.A. and Legtenberg, R. "Electrostatically driven vacuum-encapsulated polysilicon resonators: Part II. Theory and performance", *Sensors and Actuators A*, **45**, pp. 67-84 (1994).

14. Rhoads, J.F., Shaw, S.W. and Turner, K.L. "The nonlinear response of resonant microbeam systems with purely-parametric electrostatic actuation", *Journal of Micromechanics and Microengineering*, **16**, pp. 890-899 (2006).

15. Lin, W.H. and Zhao, Y.P. "Casimir effect on the pull-in parameters of nanometer switches", *Microsystem Thechnologies*, **11**, pp. 80-85 (2005).

16. Lin, W.H. and Zhao, Y.P. "Nonlinear behavior for nanoscale electrostatic actuators with Casimir force", *Chaos Solitons and Fractals*, **23**, pp. 1777-1785 (2005).

17. Lamoreaux, S.K. "The Casimir force: background, experiments, and applications", *Reports on Progress in Physics*, **68**, pp. 201-236 (2005).

18. Lifshitz, E.M. "The theory of molecular attractive forces between solids", *Soviet Physics JETP*, **2**, pp. 73-83 (1956).

19. Klimchitskaya, G.L., Mohideen, U. and Mostepanenko, V.M. "Casimir and van der Waals forces between two plates or a sphere (lens) above a plate made of real metals", *Physical Review A*, **61**, 062107 (2000).

20. Bordag, M., Mohideen, U. and Mostepanenko, V.M. "New developments in the Casimir effect", *Physics Reports*, **353**, pp. 1-205 (2001).

21. Ramezani, A., Alasty, A. and Akbari, J. "Closed-form solutions of the pull-in instability in nano-cantilevers under electrostatic and intermolecular surface forces", *International Journal of Solids and Structures*, **44**, pp. 4925-4941 (2007).

22. Yang, J., Jia, X.L. and Kitipornchai, S. "Pull-in instability of nano-switches using nonlocal elasticity theory", *Journal of Physics D Applied Physics*, **41**, p. 035103 (2008).

23. Xiao, L.J., Yang, J. and Kitipornchai, S., *Pull-in Instability of Geometrically Nonlinear Micro-Switches under Electrostatic and Casimir Forces*, Springer-Verlag, USA (2010).

24. Batra, R.C., Porfiri, M. and Spinello, D. "Vibrations and pull-in instabilities of micro electromechanical von Kármán elliptic plates incorporating the Casimir force", *Journal of Sound and Vibration*, **315**, pp. 939-960 (2008).

25. Batra, R.C., Porfiri, M. and Spinello, D. "Reduced-order models for micro electromechanical rectangular and circular plates incorporating the Casimir force", *International Journal of Solids and Structures*, **45**, pp. 3558-3583 (2008).

26. Pelesko, J. and Triolo, A. "Nonlocal problems in MEMS device control", *Journal of Engineering Mathematics*, **41**, pp. 345-366 (2001).

27. Eringen, C. "On differential equations of nonlocal elasticity and solutions of screw dislocation and surface waves", *Journal of Applied Physics*, **54**, pp. 4703-4710 (1983).

28. Ghorbanpour Arani, A., Kolahchi, R. and Mosallaie Barzoki, A.A. "Effect of material inhomogeneity on electro-thermo-mechanical behaviors of functionally graded piezoelectric rotating cylinder", *Apply Mathematical Modeling*, **35**, pp. 71-89 (2011).

29. Liang Ke, L., Sheng Wang, Y. and Dao Wang, Z. "Nonlinear vibration of the piezoelectric nanobeams based on the nonlocal theory", *Composite Structures*, **94**, pp. 2038-2047 (2012).

30. Pelesko, J.A. and Bernstein, D.H., *Modeling MEMS and NEMS*, Chapman & Hall, Boca Raton (2002).

31. Ghorbanpour Arani, A., Ghaffari, M., Jalilvand, A. and Kolahchi, R. "Nonlinear nonlocal pull-in instability of boron nitride nanoswitches", *Acta Mechanica*, **224**, pp. 3005-3019 (2013).

32. Lamoreaux, S.K. "The Casimir force: background, experiments, and applications", *Reports on Progress in Physics*, **68**, pp. 201-236 (2005).

33. Gusso, A. and Delben, G.J. "Dispersion force for materials relevant for micro- and nanodevices fabrication", *Journal of Physics D: Applied Physics*, **41**, p. 175405 (2008).

34. Israelachvili, J.N., *Intermolecular and Surface Forces*, Academic Press, London (1991).

35. Shu, C., *Differential Quadrature and Its Application in Engineering*, Springer, Berlin, German (2000).

36. Yang, J. and Xiang, H.J. "Thermo-electro-mechanical characteristics of functionally graded piezoelectric actuators", *Smart Material and Structure*, **16**, pp. 784-797 (2007).

37. Zong, Z. and Zhang, Y., *Advanced Differential Quadrature Methods*, CRC Press, New York (2009).

38. Kuang, J.H. and Chen, C.J. "Adomian decomposition method used for solving nonlinear pull-in behavior in electrostatic micro-actuators", *Mathematical and Computer Modelling*, **41**, pp. 1479-1491 (2005).

39. Wazwaz, A. "The numerical solution of sixth-order boundary value problems by the modified decomposition method", *Applied Mathematics and Computation*, **118**, pp. 311-325 (2001).

40. Wazwaz, A. "Approximate solution to boundary value problems of higher order by modified decomposition method", *Applied Mathematics and Computation*, **40**, pp. 679-691 (2000).

41. Wazwaz, A. "A reliable modification of Adomain decomposition method", *Applied Mathematics and Computation*, **102**, pp. 77-86 (1999).

Appendix A

The variables of Eq. (39) in order to obtain the deflection of BNNB can be expressed as:

$$f_A\left[\begin{array}{l} f_{A_0}=f_{A_0}\left(\bar{w}(0)\right)=A \\ f_{A_1}=\bar{w}(1)f'_A\left(\bar{w}(0)\right)=\bar{w}(1)A \\ f_{A_2}=\bar{w}(2)f'_A\left(\bar{w}(0)\right)+\dfrac{\bar{w}^2(1)}{2!}f''_A\left(\bar{w}(0)\right) \\ \qquad =\bar{w}(2)\times A+\bar{w}(1)^2\times A \\ \vdots \\ f_{A_{k+1}}=\bar{w}(k+1)f'_A\left(\bar{w}(0)\right)+\cdots \\ \qquad +\dfrac{\bar{w}^{k+1}(1)}{(k+1)!}f_A^{k+1}\left(\bar{w}(0)\right) \end{array}\right. \tag{A.1}$$

$$f_B\left[\begin{array}{l} f_{B_0}=f_{B_0}\left(\bar{w}(0)\right)=B \\ f_{B_1}=\bar{w}(1)f'_B\left(\bar{w}(0)\right)=\bar{w}(1)\times 2B \\ f_{B_2}=\bar{w}(2)f'_B\left(\bar{w}(0)\right)+\dfrac{w^2(1)}{2!}f''_B\left(\bar{w}(0)\right) \\ \qquad =\bar{w}(2)\times 2B+\bar{w}(1)^2\times 3B \\ \vdots \\ f_{B_{k+1}}=\bar{w}(k+1)f'_B\left(\bar{w}(0)\right)+\cdots \\ \qquad +\dfrac{\bar{w}^{k+1}(1)}{(k+1)!}f_B^{k+1}\left(\bar{w}(0)\right) \end{array}\right. \tag{A.2}$$

$$f_D\left[\begin{array}{l} f_{D_0}=f_{D_0}\left(\bar{w}(0)\right)=D \\ f_{D_1}=\bar{w}(1)f'_D\left(\bar{w}(0)\right)=\bar{w}(1)\times 4D \\ f_{D_2}=\bar{w}(2)f'_D\left(\bar{w}(0)\right)+\dfrac{\bar{w}^2(1)}{2!}f''_D\left(\bar{w}(0)\right) \\ \qquad =\bar{w}(2)\times 4D+\bar{w}(1)^2\times 10D \\ \vdots \\ f_{D_{k+1}}=\bar{w}(k+1)f'_D\left(\bar{w}(0)\right)+\cdots \\ \qquad +\dfrac{\bar{w}^{k+1}(1)}{(k+1)!}f_D^{k+1}\left(\bar{w}(0)\right) \end{array}\right. \tag{A.3}$$

Substituting Eqs. (A.1)-(A.3) into Eq. (39) yields:

$$\begin{aligned} \bar{w}_1(x) &= \left(\frac{B'}{2!}x^2+\frac{C'}{3!}x^3+L^{-1}(f_{A_0}) \right. \\ &\quad \left. +L^{-1}(f_{B_0})+L^{-1}(f_{D_0})\right) \\ &= \left(\frac{B'}{2!}x^2+\frac{C'}{3!}x^3+\frac{(f\times\beta+\beta+R_c)}{4!}x^4\right), \end{aligned} \tag{A.4}$$

$$\begin{aligned} \bar{w}_2(x) &= L^{-1}(f_{A_1})+L^{-1}(f_{B_1})+L^{-1}(f_{D_1}) \\ &= (A+2B+4D)\left(B'\frac{x^6}{6!}+C'\frac{x^6}{6!} \right. \\ &\quad \left. +(A+B+D)\frac{x^8}{8!}\right). \end{aligned} \tag{A.5}$$

And this procedure can be continued to reach a more accurate result. As example, for $\bar{w}_3$:

$$\begin{aligned} \bar{w}_3(x) =& L^{-1}(f_{A_2})+L^{-1}(f_{B_2})+L^{-1}(f_{D_2}) \\ =& A\left((A+2B+4D)\left(B'\frac{x^{10}}{90\times 56\times 6!} \right.\right. \\ &+ \left. C'\frac{x^{11}}{11!}+\frac{A+B+D}{12!}x^{12}\right) \\ &+ B'\frac{A+B+D}{336\times 72\times 10}x^{10} \\ &+ C'\frac{A+B+D}{720\times 144\times 11}x^{11} \\ &+ \left.\frac{(A+B+D)^2}{24^2\times 90\times 132}x^{12}\right) \\ &+ B\left(2(A+2B+4D)\left(B'\frac{x^{10}}{90\times 56\times 6!} \right.\right. \\ &+ \left. C'\frac{x^{11}}{11!}+\frac{A+B+D}{12!}x^{12}\right) \\ &+ B'\frac{A+B+D}{112\times 72\times 10}x^{10} \\ &+ C'\frac{A+B+D}{240\times 144\times 11}x^{11} \\ &+ \left.\frac{(A+B+D)^2}{24^2\times 30\times 132}x^{12}\right) \\ &+ D\left(4(A+2B+4D)\left(B'\frac{x^{10}}{90\times 56\times 6!}\right.\right. \end{aligned}$$

$$+ C' \frac{x^{11}}{11!} + \frac{A+B+D}{12!} x^{12} \Bigg)$$
$$+ B' \frac{A+B+D}{336 \times 72} x^{10}$$
$$+ C' \frac{A+B+D}{24 \times 144 \times 11} x^{11}$$
$$+ \frac{(A+B+D)^2}{24^2 \times 9 \times 132} x^{12} \Bigg). \tag{A.6}$$

Biographies

Ali Ghorbanpour Arani received his B.Sc. degree from Sharif University of Technology, Tehran, Iran, in 1988. He then received his M.Sc. degree from Amirkabir University of Technology, Tehran, Iran, in 1991 and his Ph.D. degree from the Esfahan University of Technology, Esfahan, Iran, in 2001. Dr Ali Ghorbanpour Arani is a Professor in the Mechanical Engineering Faculty of University of Kashan, Kashan, Iran. He has authored more than 129 refereed journal papers and 10 books. His current research interests are stress analyses, wave stress propagation, stability and vibration of nano-tubes, nano-composite and functionally graded materials.

Abdolreza Jalilvand received his B.Sc. degree from the Imam Khomeini International University in Qazvin, Iran, in 2011. He then received his M.Sc. degree from University of Kashan in Kashan, Iran, in 2013. His research interests are vibration, nano and micro electromechanical systems and instability of smart materials.

Mahdi Ghaffari received his B.Sc. degree from the Isfahan University of Technology, Iran, in 2011. He then received his M.Sc. degree from University of Kashan, Iran, in 2014. His research interests are nano/micro electromechanical systems, nonlinear vibration and numerical solution methods. He currently works on simulation MEMs/NEMs with finite element software.

Mohsen Talebi Mazraehshahi received his B.Sc. degree from the Islamic Azad University, Kashan branch in Kashan, Iran, in 2010. He is currently an M.Sc. student at University of Kashan in Kashan, Iran. His research interests are vibration and instability of smart materials.

Reza Kolahchi received his B.Sc. degree from the Islamic Azad University, Kashan branch in Kashan, Iran, in 2009. He then received his M.Sc. degree from University of Kashan in Kashan, Iran, in 2011. He is currently a Ph.D. student at University of Kashan in Kashan, Iran. He has authored 40 refereed journal papers. His research interests are nano-mechanics, vibration, buckling and instability of smart materials.

Mir Abbas Roudbari received his B.Sc. degree from the University of Shahid Bahonar Kerman, Iran, in 2006. He then received his M.Sc. degree from University of Guilan, Iran, in 2009. He is currently a Ph.D. student at University of Kashan, Iran. His research interests are vibration, wave propagation and buckling analyses of carbon and boron nitride nanotubes and smart materials.

Saeed Amir received his B.Sc. degree from the University of Kashan in Kashan, Iran, in 2007. He then received his M.Sc. degree from University of Kashan in Kashan, Iran, in 2009. He is currently a Ph.D. student at University of Kashan in Kashan, Iran. He has authored 34 refereed journal papers. His research interests are bio-mechanics, FGM, vibration and instability of nano-composite materials.